

An Efficient Machine Learning Approach for Prediction of Conjunctiva Hyperemia Assessment using Feature Extraction Methods

Savita Bamal* and Latika Singh

School of Engineering & Technology, Sushant University, Gurgaon - 122018, Haryana,
Email: *Savita.phd19@sushantuniversity.edu.in , Latikaduhan@sushantuniversity.edu.in

Abstract: The human eye is one of the most intricate sense organs. It is crucial to protect your eyes against several eye disorders that can cause vision loss if untreated in order to maintain your ability to see well. Early detection of eye diseases is therefore crucial in order to prevent any unintended consequences and control the diseases continued progression. Conjunctivitis is one such eye condition that is characterized by conjunctival inflammation, resulting in symptoms like hyperemia (redness) due to increased blood flow. With the aid of the best treatments, modern techniques, and early, precise diagnosis by professionals, it can be cured or can be greatly reduced. The proper diagnosis of the underlying cause of visual problems is frequently postponed or never carried out because of shortage of diagnostic experts, which leads to either insufficient or postponed corrective treatment. In order to diagnose and evaluate conjunctivitis, segmentation methods are essential for locating and measuring hyperemic regions. In the present study, segmentation techniques are applied along with feature extraction techniques to provide an effective machine learning framework for the prediction of eye problems. Using the discrete cosine transform (DCT), the segmented regions of interest are converted into feature vectors. These feature vectors are then used to train machine learning classifiers, including random forest and neural networks, which achieve a promising accuracy of 95.92%. This approach enables ophthalmologists to make more objective and accurate assessments, aiding in disease severity evaluation.

Keywords: Conjunctival Hyperemia, Segmentation, Otsu's Thresholding, Morphological operation, Segmentation Process, Feature extraction, Machine Learning, Random Forest.

1. INTRODUCTION

The human eye is one of the most complex sensory organs. If you want to keep your vision sharp, it's critical for you to protect your eyes against a number of ailments that can damage them and impair eyesight if left untreated. Early detection and monitoring of eye diseases is essential for preventing further disease progression. Hyperemia refers to an increased blood flow to a particular tissue or organ, which causes redness and warmth in the affected area. There are many causes of hyperemia. Situations that are either chronic or acute usually produce hyperemia. The disease's first stage is characterized by redness, burning, or tearing in the sclera portion. The density and area occupied by the red lesions determine severity of the disease (Figure 1).



Fig. (1): Conjunctival image

This condition, also known as hyperemia, erythema, or conjunctival injection, can be thoroughly evaluated to rule out other potential causes such as contact lens problems, allergies, or dry eye [2][3]. Additionally, evaluating the growth rate and response to treatments is crucial. Timely diagnosis of conjunctivitis is vital for effective therapy and preserving eyesight. However, in developing nations, like India the population-to-ophthalmologist ratio is significantly imbalanced, with ratios as low as 1:25000 in urban areas and 1:219000 in rural areas [4]. This scarcity of healthcare practitioners makes it challenging to cater to large populations, but advancements in technology offer a promising solution for

screening eye issues such as conjunctiva hyperemia. Therefore, it is suggested to develop an effective model to predict eye diseases using machine learning (ML) and segmentation followed by feature extraction techniques, in order to help with accurate diagnosis. The first objective is to forecast specific region of interest of diseased and normal eye (region of interest) using segmentation approach followed with feature extraction methods, and machine learning (ML) techniques. Appropriate traditional ML techniques, including Random Forest (RF) and Neural Net (NN), were chosen for application of ML techniques. In the case of conjunctivitis hyperemia, segmentation and supervised learning approaches aim to delineate and isolate the hyperemic areas within the conjunctiva using various image processing techniques and algorithms, which leverages the distinct red color of hyperemic conjunctiva compared to healthy areas. Efficient computer vision algorithms are crucial in addressing these challenges of hyperemia classification. Once the hyperemic regions are successfully segmented, further analysis and quantification can be performed, such as measuring the percentage of conjunctival area affected by hyperemia or assessing the severity based on the extent of redness. Machine Learning approaches play a critical role in the analysis and assessment of conjunctivitis hyperemia by providing accurate information for diagnosis, monitoring, and treatment evaluation, thereby enhancing the screening of conjunctivitis.

The rest of the paper is structured as follows: A brief summary of many research that were used to develop segmentation strategies and feature extraction techniques for conjunctival hyperemia is provided in Section 2. Section 3 explains the fundamental workflow procedure for obtaining ROI of diseased and healthy eyes as well as the feature extraction method utilizing DCT. Section 4 explains how to use the DCT method to extract features from segmented images. Section 5 describes the two classifiers Random Forests and Neural Networks. Section 6 discusses the results and provides accuracy information. Conclusion and the area of future work are described in the final section.

2. RELATED WORK

Although further model developments are necessary before using a highly effective and robust classifier tool in clinical practices, the development of computer assisted diagnosis is still an active research topic. Prior to allowing for medical practices, the primary problems associated with medical picture screeners necessitate many tests. There is a review of the literature in this part that briefly discusses the studies related to computer based hyperemia eye redness detecting system. Earlier work has shown clinical and grading scale methods for the diagnosis of diseased eyes [1], but these methods were

found to be very time-consuming and less reliable. Researchers have proposed several manual and semi-automated segmentation approaches to detect red lesions [2]. Many segmentation approaches have been developed, including image pixel-based, color-based, edge-based, region-based, or texture-based methods [2]. Human eye redness grading [2] is detected using a partial automated method named canny edge detection, where segmentation were used to isolate the sclera region. However, the computation time is a concern in such cases where pixel-based iteration is required [2]. A fuzzy Canny method has been used for detecting edges of the image [3] [4], and subsequently, morphological operations were applied for segmentation to achieve better results [4]. [5] used a Bayesian classifier to perform image analysis, focusing on two primary aspects of redness and the appearance of blood vessels. However, segmentation still relied on human trials in medical practice [5]. Multiple image segmentation models have been explored by numerous research groups, employing techniques such as thresholding, color extraction, and edge detection [6].

In the context of ocular scanning for disease detection, Laddi *et.al.* [7] set up a relatively expensive and intricate computer vision system. They utilized the Adaptive Neural Fuzzy Inference System (ANFIS) and RGB values for classification, claiming 90% accuracy in disease detection. Zhou *et al.* [8] provided a thorough sclera image quality measure for sclera detection, determining the authenticity of the image, evaluating its quality, analyzing the correctness of segmentation, and assessing whether it contains enough feature information for recognition. Sclera vein pattern improvement using multiple directional Gabor filters was also demonstrated to increase the effectiveness of sclera recognition. Kaya *et.al.* [9] demonstrated a pattern stabilization technique for use in laser eye surgery, which employed features extracted from scleral blood vessels to track the patient's eye pattern of red lesions. This method created a mask using the Hough transform and RANSAC algorithm to reflect the ablation pattern, and SIFT technique was applied to the entire image for reducing the number of important points and eliminating edge effects. Wu and Harada [10] proposed algorithms for the extraction of blood vessels from photographs of the sclera and conjunctiva. They predicted an innovative pseudo vessel removal approach to remove noise and used Otsu's method to automatically determine the threshold value. The original strategy utilized the branching characteristics of blood vessels for blood vessel extraction in the sclera conjunctiva region. The sclera was subjected to the Graph Cut segmentation algorithm [11], and a rectangular mask was utilized to precisely eliminate the borders of the eyelids. The dimensions of the rectangle were chosen such that its height equaled its circumference.

Despite the continuous development and research of conjunctiva scanning image processing models, more research exploration is required to develop an automated computer-aided screener for conjunctiva hyperemia eye disease detection.

The accuracy of segmentation plays a vital role in efficient screener development. The presented ML model for conjunctivitis classification may represent a breakthrough in the accurate grading of machine-based automated screening models. Although, the current study has contributed to establishing the conjunctival hyperemia measurement system, a highly reliable and subject-independent system still requires

further attention. The current study aims to partially reduce this gap by extracting features from ROI-based images and developing machine learning algorithms that can classify between a normal eye and an eye with conjunctivitis. The approach used for the current work is discussed in the following section.

3. METHODOLOGY USED

The complete segmentation and classification process, based on machine learning algorithms, is illustrated in Figure 2, a flowchart that depicts the step-by-step workflow of the proposed methodology.



Fig (2): Proposed Methodology

Image segmentation is a crucial part to develop an efficient eye disease screening model in this study. In this proposed work, fifty images with bulbar redness and thirty healthy eyes images were used. The images were obtained from vision lab at School of Health Sciences. The three-step slit lamp process was used to acquire the images using HUVITZ 500N and CANON EOS 1300D camera (linked with the system itself). The typical sample images are shown in Figure 3a and 3b.



Fig. (3a): Diseased eye image



Fig. (3b): Healthy eye image

After extracting the ROI, the segmented image needs to be processed through machine learning models for feature extraction and classification. Using segmented (ROI) images as inputs in machine learning models yields superior results compared to directly using raw data images, thereby achieving better accuracy. In the case of Hyperemia conjunctivitis disease, the sclera serves as the region of interest for red lesion grading. The proposed process is illustrated in Figure 4, as shown in the flowchart.

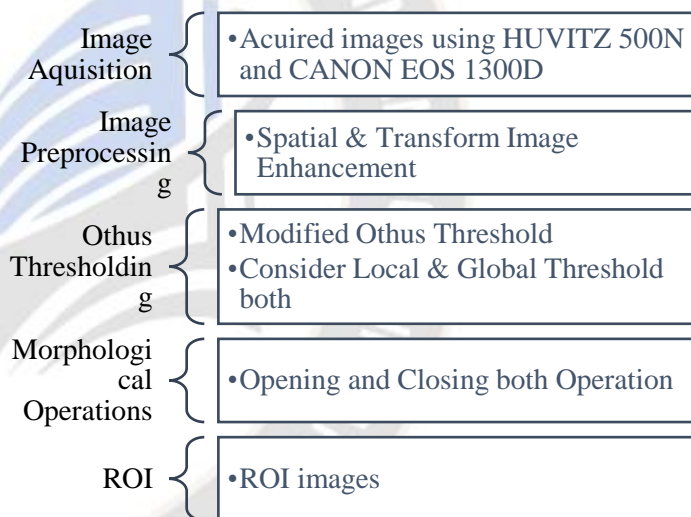


Fig. (4): Flowchart of Proposed Segmentation Process

Since the images were acquired manually, preprocessing techniques are employed to remove noise and other irrelevant areas in the image that are not necessarily required for disease grading. During image cleaning process, spatial and transform-based approaches are considered to enhance the image. Initially, color map changes are applied to convert RGB color images into grayscale images, and a suitable threshold is sought to distinguish the sclera region from other regions in the raw images, such as eyelids, skin, and the pupil. Otsu's thresholding approach is still widely considered optimal in most cases [12].

A modified Otsu's thresholding technique is utilized to obtain the global threshold value on a 2D image array. This iterative-based method aims to find the minimal variances between two

groups of pixels. The algorithm iteratively searches for the threshold that minimizes the variation within each class. The within-class variance is defined as the weighted sum of the variances of the two classes (foreground and background pixel groups). By continuously refining the threshold, the algorithm minimizes the within-class variance, effectively separating the foreground and background pixel groups

The following equation is used to calculate the within class variance in threshold T

$$\sigma^2(T) = P_F^2(T)\sigma_F^2(T) + P_B^2(T)\sigma_B^2(T) \dots \dots \dots (1)$$

Where P_F and P_B represents the probability of the pixels in foreground and background regions at the threshold T, σ_F & σ_B represent foreground & background variance in the respective group of the pixels in gray image. The P_F and P_B can be calculated in as per equations 2.

$$P_F = \frac{\text{Pixels counts in Foreground}}{\text{Total Pixels}} \dots \dots \dots (2)$$

$$P_B = \frac{\text{Pixels counts in Background}}{\text{Total Pixels}} \dots \dots \dots (3)$$

The variance is calculated as

$$\sigma = \frac{\sum(x-v)}{N} \dots \dots \dots (4)$$

x is the pixels; v is the mean of the pixels in the particular group (foreground or background) and N is the total number of all pixels. Once getting the optimal threshold value, the image is classified in two regions (sclera and non-sclera part). The Otsu's approach has applied in the following sample matrix better clarification in figure 5, LHS represent the Original Matrix and RHS shown the result using Otsu's method.

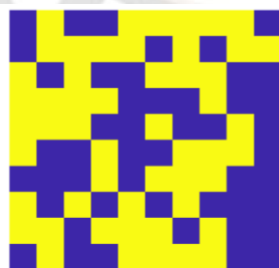
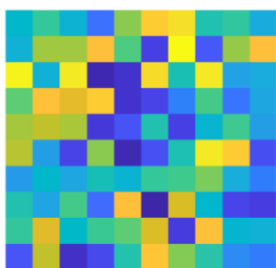


Fig (5a): LHS- Original Matrix Fig (5b): RHS Segment scale color

Subsequently, the resulting image underwent morphological operations to further enhance the accuracy of the segmentation results. The specific steps implemented in the morphological operations can be seen in Figure 6.

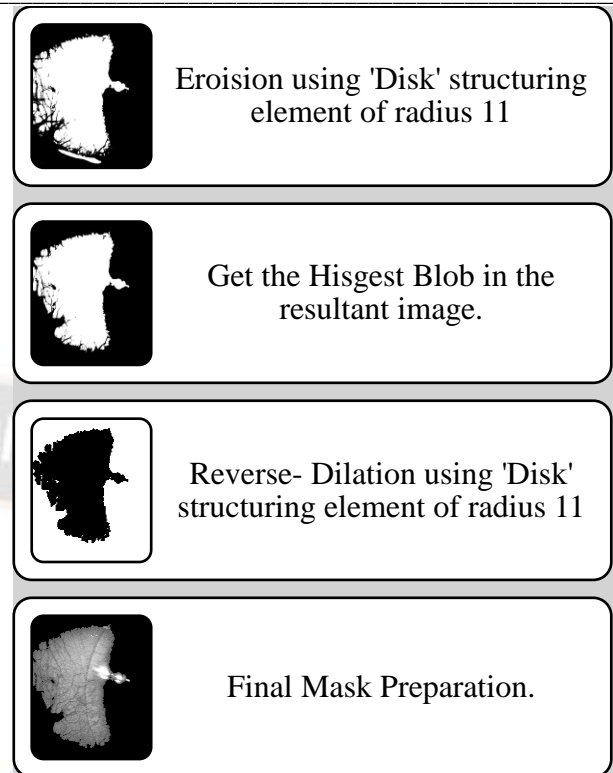


Fig. (6): Morphological Operations Steps

In Figure 7 and 8, detailed sample segmented ROI results of 30 images are displayed, along with the corresponding raw images, providing an assessment of the accuracy achieved by the proposed method.

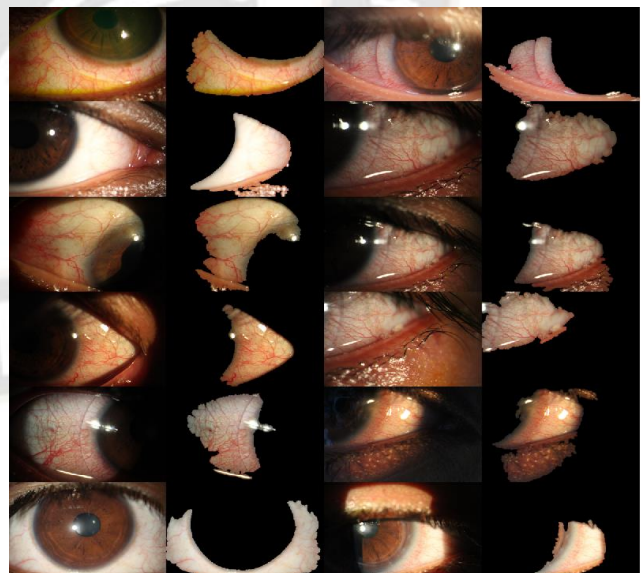


Fig (7): Segmented (ROI) result Images

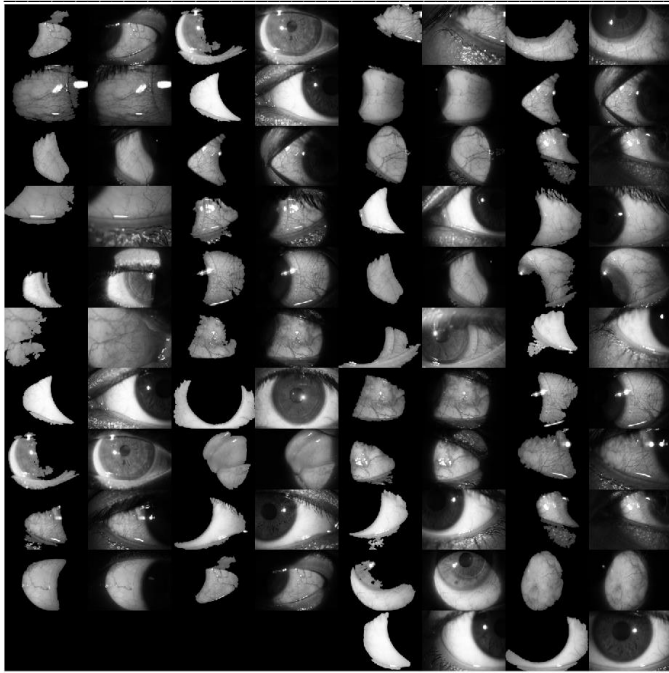


Fig (8): ROI Result images

4. Feature Extraction and Classification:

Feature extraction is the process of selecting and transforming relevant data from a dataset to highlight key patterns or characteristics, often employed as a crucial step in machine learning.

To classify segmented images, firstly the feature data matrix is prepared using discrete cosine transform. This feature matrix is used as training data for classifier to compute accuracy for differentiating eyes with conjunctivitis and normal eyes. This process is described in section 4.1 and section 4.2.

4.1 Feature extraction of ROI images using DCT transformation:

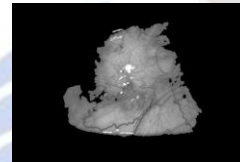
DCT is a mixture of sinusoids with various magnitudes and frequencies, the discrete portrays an image. A few DCT coefficients include all of the crucial visual characteristics in a DCT transformed image. Each block in the DCT transform image is known as a basis function, where the horizontal frequency grows from right to left and the vertical frequency increases from top to bottom. The first black block signifies the image's DC coefficients. With DCT cosine coefficients, the 2D DCT transformation represents the image's visually important information properties. Equation 5 defines the 2D DCT transformation equation of the N by M image, where $f(i,j)$ denotes the spatial domain and $F(u,v)$ denotes the transformed domain image [13].

$$F(u, v) = \sqrt{\frac{2}{N}} \cdot \sqrt{\frac{2}{M}} \sum_{i=0}^{N-1} \sum_{j=0}^{M-1} f(i, j) \cdot \cos \left[\frac{\pi \cdot u}{2 \cdot N} (2i + 1) \right] \cdot \cos \left[\frac{\pi \cdot v}{2 \cdot M} (2j + 1) \right] \cdot f(i, j) \dots (5)$$

Algorithm: Below given steps explain process of feature extraction with 2D DCT method.

1. Apply segmentation approach on raw eye images to find ROI as explained in section 3.
2. Read gray scale ROI images obtained from step 1.
3. Apply 2D DCT transformation on each block (Block size 8*8), which converts the pixel values into a set of DCT coefficients. All segmented images (ROI) features are represented as a row matrix using the discrete cosine transform (DCT), with higher coefficients ignored as shown in Figure 9 b.
4. After DCT, inverse DCT of ROI images is computed in Figure 9c.

9.(a): ROI image



9.(b):DCT of ROI image



9.(c):InverseDCT of ROI image



5. Once the feature data matrix is prepared, a labeled dataset is created.

Each segmented image is associated with a corresponding class label, distinguishing between red lesioned images and normal images. The dataset is then split into training and testing subsets. The selected DCT features and their corresponding class labels are fed into a machine learning classifier. It is crucial to choose a classifier that is appropriate for the number of features and the size of the dataset, such as, Random Forest and Neural Networks.

4.2 Classification:

The next step involves training the classifier using the training subset, enabling it to learn the patterns and relationships between the DCT features and their corresponding class labels. After training, the classifier is evaluated using the testing subset. To optimize the model and measure classification

performance, metrics such as accuracy, precision, recall are calculated.

A neural network uses a cascade of neural layers to train the network according to the design specifications. The input layer applies the input feature matrix, and the decision node gets the outcome based on learning weight factors. The proposed neural net classifier tested the model over 50 iterations with a learning rate of 0.01.

Another classifier that results the creation of decision tree classifiers using the random forest technique is becoming increasingly popular. Each tree generates a random vector based on an independent set of data. The probability distribution is the same for all randomly generated tree vectors. The classifier model uses 100 trees, a gain ratio of 1, and a maximum depth of 10 [14].

The results are explained in next section.

6. Performance Metrics:

The performance of the classifier depends on the input samples that the classification model properly or erroneously predicts. Accuracy, precision, and recall are performance indicators that track each classification step. To assess the performance of the used ML algorithms, the widely used measuring tools of recall, accuracy, and precision are used in this study. There are many studies that have already used these measurement indices, including [15][16]. The classification of the disorders as positive or negative is considered as normal. The measurements were produced using Equations (6) through (8).

Accuracy: It is only the proportion of accurately predicted cases to all instances. Equation 6[15] illustrates it.

$$Accuracy = \frac{Correctly\ predicted\ instances}{Total\ number\ of\ input\ instance} \dots \dots (6)$$

Precision: It is ratio of correctly classified positive examples to total number of classified positive instances(either correctly or incorrectly). It appears in equation 7 [15].

$$Precision = \frac{Correct\ positive\ instances}{total\ number\ of\ classified\ positive\ instances(either\ correctly\ or\ incorrectly)} \dots \dots (7)$$

Recall: It represents the percentage of positive instances that the classifier accurately predicted. Equation 8 illustrates it [15].

$$Recall = \frac{correctly\ predictive\ positive\ instances}{True\ positive\ instances} \dots \dots (8)$$

By utilizing the frequency information provided by the DCT features, this classification approach enables the identification of hyperemic regions or other segmented areas of interest in the images.

Results and Discussion:

The classifier is trained and tested using a locally acquired images, images that were collected using the slit lamp technique. After that images are segmented using morphological methods and once the feature vector is extracted using DCT on ROI images, further fed this feature vector in classifiers to build the model. The proposed model is tested with 50 diseased images and 50 healthy images using neural net and random forest classifiers. An accuracy of 96% with random forest and 94% accuracy with neural network is achieved. It is apparent that the Random Forest, with 50 features, provides the best accuracy (96%) for the current feature set shown in Figure 10.

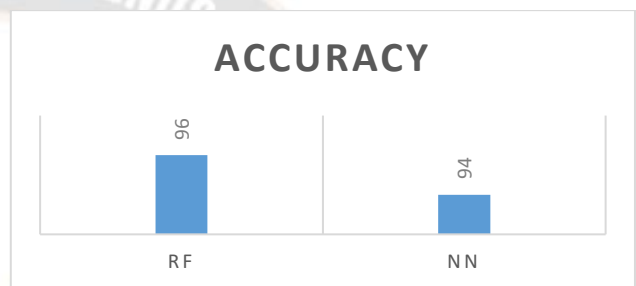


Fig (10): Accuracy computer with RF and NN classifiers

The detailed comparison results of accuracy with or without ROI on raw images are depicted in Figure 11.and results are also shown in bar plots.

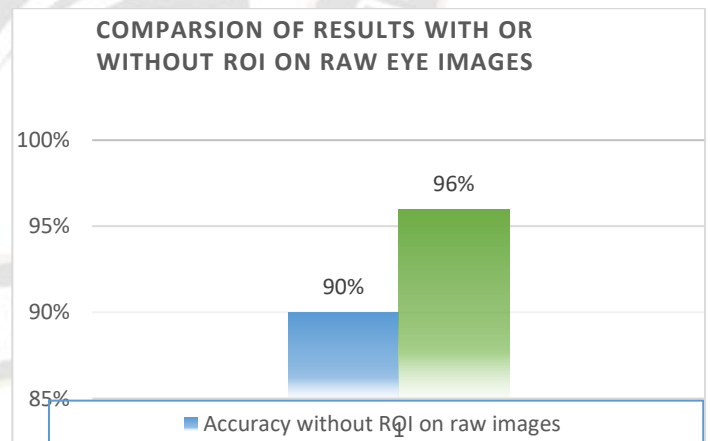


Fig (11): Accuracy comparison

5. CONCLUSION:

Hyperemia conjunctivitis, characterized by redness and swelling of the conjunctiva, can be effectively detected using image processing-based machine learning (ML) models. While most ML-based image screeners rely on raw images for disease quantification or apply algorithms to segmented images to enhance accuracy, the present work focuses on the development of a segmentation model for screening conjunctiva hyperemia eye diseases with machine learning classification algorithm using feature extraction. Otsu's thresholding and morphological operations to obtain accurate segmentation results are applied. Subsequently, feature extraction using Discrete Cosine Transform (DCT) coefficients was performed on the segmented regions, and the resulting feature data was fed into a machine learning classifier.

The proposed approach achieved an accuracy of 96%, Recall for red eyes 95% and Precision for red eyes 87% using Random Forest and Neural Network classifiers. This segmentation with feature extraction methodology generally outperforms direct feature extraction models. By combining segmentation techniques with feature extraction and employing machine learning algorithms, potential to greatly enhance the accuracy and efficiency of grading and managing hyperemia conjunctivitis images is demonstrated.

In conclusion, the proposed work offers promising advancements in the field of hyperemia conjunctivitis detection. By leveraging image processing-based ML models and incorporating segmentation and feature extraction techniques, significant accuracy improvement is achieved, paving the way for more accurate and efficient grading and management of hyperemia conjunctivitis images.

Acknowledgement:

The authors sincerely acknowledged the vision center under department of optometry, School of Health Sciences, Sushant University, Gurugram for facilitating to acquired images and clinical advice.

REFERENCES

- [1] L. J. K. Lens Al , Coyne Sheila Nemeth, *Ocular Anatomy and Physiology*, Illustrate. SLACK Incorporated, 2008.
- [2] M. M. Schulze, D. A. Jones, and T. L. Simpson, "The development of validated bulbar redness grading scales," *Optom. Vis. Sci.*, vol. 84, no. 10, pp. 976–983, 2007, doi: 10.1097/OPX.0b013e318157ac9e.
- [3] P. Fieguth and T. Simpson, "Automated measurement of bulbar redness," *Investig. Ophthalmol. Vis. Sci.*, vol. 43, no. 2, pp. 340–347, 2002.
- [4] M. W. Khan, "Technology & Research Diabetic Retinopathy Detection using Image Processing : A Survey," vol. 1, no. 1, 2013.
- [5] H. Narasimha-Iyer *et al.*, "Robust detection and classification of longitudinal changes in color retinal fundus images for monitoring diabetic retinopathy," *IEEE Trans. Biomed. Eng.*, vol. 53, no. 6, pp. 1084–1098, 2006, doi: 10.1109/TBME.2005.863971.
- [6] J. S. Wolffsohn and C. Purslow, "Clinical monitoring of ocular physiology using digital image analysis," *Contact Lens Anterior Eye*, vol. 26, no. 1, pp. 27–35, 2003, doi: 10.1016/S1367-0484(02)00062-0.
- [7] A. K. Amit Laddi, "Intelligent Machine Vision Technique for Disease Detection through Eye Scanning," in *Case Studies in Intelligent Computing*, Auerbach Publications, 2014, p. 24.
- [8] Z. Zhou, E. Y. Du, N. L. Thomas, and E. J. Delp, "A comprehensive approach for sclera image quality measure," *Int. J. Biom.*, vol. 5, no. 2, pp. 181–198, 2013, doi: 10.1504/IJBM.2013.052972.
- [9] A. Kaya, A. B. Can, and H. B. Çakmak, "Designing a pattern stabilization method using scleral blood vessels for laser eye surgery," *Proc. - Int. Conf. Pattern Recognit.*, pp. 698–701, 2010, doi: 10.1109/ICPR.2010.176.
- [10] X. Y. Wang, Z. F. Wu, L. Chen, H. L. Zheng, and H. Y. Yang, "Pixel classification based color image segmentation using quaternion exponent moments," *Neural Networks*, vol. 74, pp. 1–13, 2016, doi: 10.1016/j.neunet.2015.10.012.
- [11] C. Rother and A. Blake, "' GrabCut ' — Interactive Foreground Extraction using Iterated Graph Cuts," vol. 1, no. 212, pp. 309–314, 2004.
- [12] N. Otsu, "'A Threshold Selection Method from Gray-Level Histograms.,"" *IEEE Trans. Syst. Man. [Cybern.*, vol. 9, no. 1, pp. 62–66, 1979.
- [13] S. Dabbaghchian, M. P. Ghaemmaghami, and A. Aghagolzadeh, "Feature extraction using discrete cosine transform and discrimination power analysis with a face recognition technology," *Pattern Recognit.*, vol. 43, no. 4, pp. 1431–1440, 2010, doi: 10.1016/j.patcog.2009.11.001.
- [14] V. Rajyaguru, C. Vithalani, and R. Thanki, "ORIGINAL RESEARCH A literature review: various learning techniques and its applications for eye disease identification using retinal images," *Int. J. Inf. Technol.*, 2020, doi: 10.1007/s41870-020-00442-8.
- [15] P. Ghosh *et al.*, "Efficient prediction of cardiovascular disease using machine learning algorithms with relief and lasso feature selection techniques," *IEEE Access*, vol. 9, pp. 19304–19326, 2021, doi: 10.1109/ACCESS.2021.3053759.
- [16] A. Al Marouf, M. M. Mottalib, R. Alhaji, J. Rokne, and O. Jafarullah, "An Efficient Approach to Predict Eye Diseases from Symptoms Using Machine Learning and Ranker-Based Feature Selection Methods," *Bioengineering*, vol. 10, no. 1, 2023, doi: 10.3390/bioengineering10010025.